

Supporting information

Aqueous nanofibers with switchable chirality formed of self-assembled dumbbell-shaped rod amphiphiles

Zhegang Huang, Eunji Lee, Ho-Joong Kim, and Myongsoo Lee*


Center for Supramolecular Nano-Assembly and Department of Chemistry
Seoul National University, Seoul 151-747, Korea

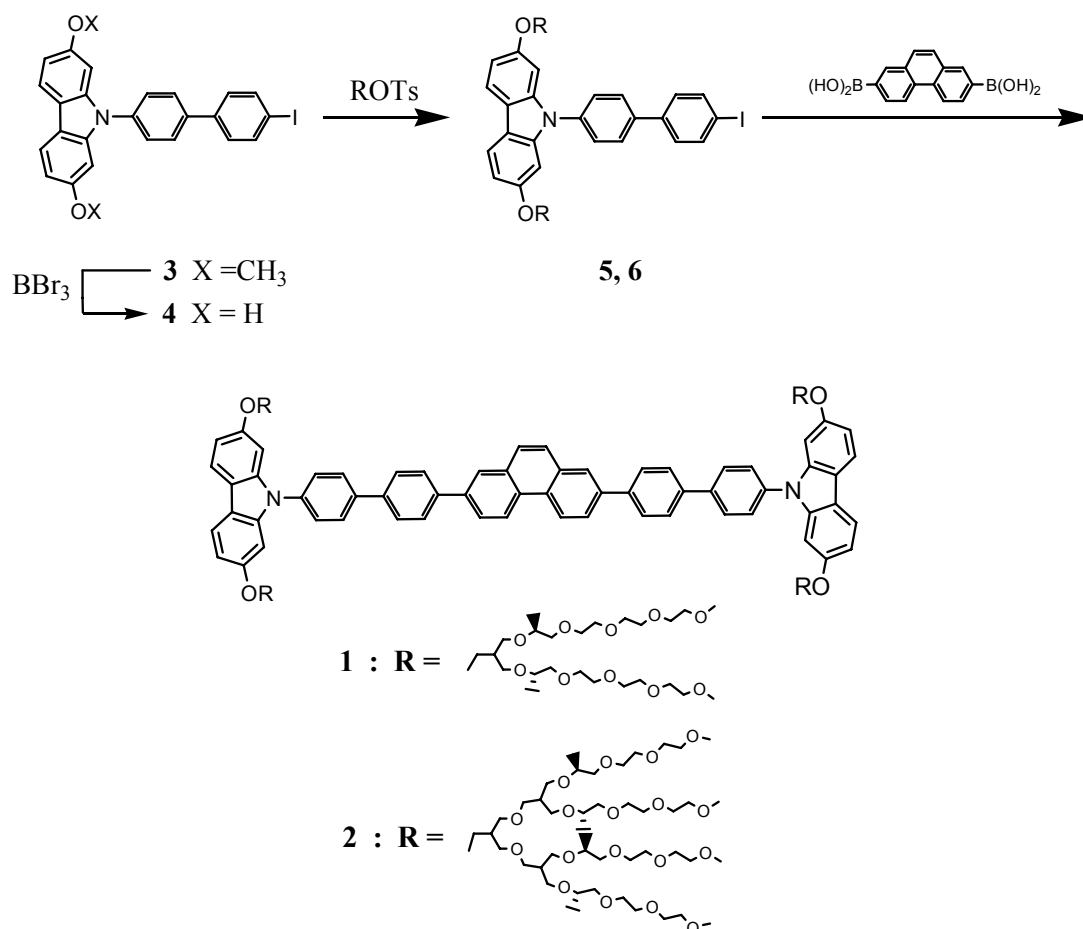
*To whom all correspondence should be addressed.

Fax 82-2-393-6096; Tel 82-2-880-4340; E-mail myongslee@snu.ac.kr

Experimental section

Materials. Benzyl bromide, NaH (60%), and *p*-toluenesulfonyl chloride (98%) from Tokyo Kasei were used as received. phenanthrene from Lancaster was used as received. Unless otherwise indicated, all starting materials were obtained from commercial suppliers (Aldrich, TCI, and Lancaster) and were used without purification. Dry THF was obtained by vacuum transfer from sodium and benzophenone. The synthetic procedure used in the preparation of the dumbbell-shaped molecules is described in scheme S1. Compound **3** and oligo-ethylene oxide segments were synthesized according to the procedures described previously.⁽¹⁾

Techniques. ¹H-NMR spectra were recorded from CDCl₃ or DMSO solutions on a Bruker AM 250 spectrometer. Dynamic light scattering (DLS) measurements were performed using an ALV / CGS-3 Compact Goniometer System. UV/vis absorption spectra were obtained from a Shimadzu 1601 UV spectrometer. The fluorescence spectra were obtained from a Hitachi F-4500 fluorescence spectrometer. Circular dichroism (CD) spectra were obtained using JASCO J-810 spectropolarimeter. Transmission electron microscope (TEM) was performed at 120 kV using JEOL-JEM 2010. MALDI-TOF-MS was performed on a Perseptive Biosystems Voyager-DE STR using a 2,5-dihydroxy benzoic acid matrix. Preparative high performance liquid chromatography (HPLC) was performed at room temperature using a 20 mm  600 mm poly styrene column on a Japan Analytical Industry Model LC-908 recycling preparative HPLC system, equipped with UV detector 310 and RI detector RI-5. Molecular modeling and mechanical calculations were computed with Materials Studio Modeling 4.0 (Accelrys Inc.) software.



Scheme S1. Synthesis of dumbbell-shaped molecules **1** and **2**.

Synthesis of Compound **4**

To a solution of compound **3** (1.24 g, 2.45 mmol) in methylene chloride at 0 °C was added 1.0 M solution of BBr₃ (15 ml). The reaction mixture was stirred at room temperature under nitrogen for 6 h. The solution was then quenched with MeOH. The resulting solution was washed with water and the solvent was removed in a rotary evaporator. The crude product was purified by column chromatography (silica gel) using ethyl acetate: hexane (1:1 v/v) to yield 1.1 g (94 %) of a white powder. ¹H-NMR (250 MHz, DMSO, δ, ppm) 9.36 (s, 2H, ArOH), 7.89 (m, 6Ar-H), 7.6 (m, 4Ar-H), 6.69 (m, 4 Ar-H).

Synthesis of compound **5** and **6**

Compound **5** and **6** were synthesized by using the same procedure. A representative example is described for **5**. Compound **4** (0.12 g, 0.25 mmol), ROTs (0.35 g, 0.52 mmol) and excess K₂CO₃ were dissolved in 30 ml of anhydrous acetonitrile. The mixture was refluxed for 24 h. The resulting solution was then poured into water and then extracted with methylene chloride. The methylene chloride solution was washed with water, dried over anhydrous magnesium sulfate, and filtered. The solvent was removed in a

rotary evaporator, and the crude product was purified by column chromatography (silica gel) using ethyl acetate/ methanol (20:1 v/v) to yield 0.22 g (68 %) of a waxy solid.

5 yield 68 %; $^1\text{H-NMR}$ (250 MHz, CDCl_3 , δ , ppm) 7.87 (d, 2Ar-H, *o* to I, 8.8 Hz), 7.77 (m, 4Ar-H), 7.59 (d, 2Ar-H, *m* to OCH_2 , 8.5 Hz), 7.45 (d, 2Ar-H, *m* to I, 8.8Hz), 6.86 (m, 4Ar-H), 4.03 (d, 4H, $2 \times \text{CH}_2\text{Ophenyl}$, $J = 3.5$ Hz), 3.67-3.36 (m, 68H, OCH_2), 3.35 (s, 12H, OCH_3), 2.52-2.24 (m, 2H, $2 \times \text{CH}(\text{CH}_2)_3$), 1.06–1.17 (m, 12H, $4 \times \text{CHCH}_3$).

6 yield 72 %; $^1\text{H-NMR}$ (250 MHz, CDCl_3 , δ , ppm) 7.87 (d, 2Ar-H, *o* to I, 8.8 Hz), 7.77 (m, 4Ar-H), 7.59 (d, 2Ar-H, *m* to OCH_2 , 8.5 Hz), 7.45 (d, 2Ar-H, *m* to I, 8.8Hz), 6.86 (m, 4Ar-H), 4.01 (d, 4H, $2 \times \text{CH}_2\text{Ophenyl}$, $J = 3.5$ Hz), 3.63-3.36 (m, 120H, OCH_2), 3.34 (s, 24H, OCH_3), 2.54-2.22 (m, 2H, $2 \times \text{CH}(\text{CH}_2)_3$), 1.92-2.15 (m, 4H, $4 \times \text{CH}(\text{CH}_2)_3$), 1.04–1.12 (m, 24H, $8 \times \text{CHCH}_3$).

Synthesis of compound 1 and 2

Compounds **1** and **2** were synthesized by using the same procedure. A representative example is described for **1**. Compound **5** (0.21 g, 0.145 mmol) and phenanthren-2,7-diyl-2,7-diboronic acid (19.3 mg, 0.072 mmol) were dissolved in degassed THF (25 ml). Degassed 2 M aqueous solution of Na_2CO_3 (25 ml) was added to the solution and then tetrakis (triphenylphosphine) palladium(0) (5 mg, 0.004 mmol) was added. The mixture was refluxed for 24 h with vigorous stirring under nitrogen. Cooled to room temperature, the layers were separated, and the aqueous layer was then washed twice with methylene chloride. The combined organic layer was dried over anhydrous magnesium sulfate and filtered. The solvent was removed in a rotary evaporator, and the crude product was purified by column chromatography (silica gel) using ethyl acetate/ methanol (10:1 v/v) as eluent and by prep. HPLC to yield 83 mg (40 %) of a waxy solid.

1 yield 40 %; $^1\text{H-NMR}$ (250 MHz, CDCl_3 , δ , ppm) 8.84 (d, 2Ar-H, 8.7 Hz), 8.24 (s, 2Ar-H), 8.07-7.78 (m, 20Ar-H), 7.65 (d, 4Ar-H, *m* to OCH_2 , 8.5 Hz), 6.86 (m, 8Ar-H), 4.06 (d, 8H, $4 \times \text{CH}_2\text{Ophenyl}$, $J = 4.9$ Hz), 3.64-3.49 (m, 136H, OCH_2), 3.36 (m, 24H, OCH_3), 2.37-2.31 (m, 4H, $\text{phenylOCH}_2\text{CH}(\text{CH}_2\text{O})_2$), 1.13–1.08 (m, 24H, $8 \times \text{CHCH}_3$); $^{13}\text{C-NMR}$ (60 MHz, CDCl_3 , ppm) : = 157.9, 142.2, 139.9, 139.8, 139.6, 132.6, 132.4, 128.7, 127.7, 127.6, 126.5, 119.0, 117.2, 108.2 95.2, 71.7, 70.8, 70.5, 69.7, 69.4, 66.5, 59.1, 40.2, 17.30; Anal. Calcd for $\text{C}_{156}\text{H}_{232}\text{N}_2\text{O}_{44}$: C, 66.27; H, 8.17; N, 0.98. Found C, 65.98; H, 8.22; N, 1.04. MALDI-TOF-MS m/z (M+H)⁺ 2863.5, (M+Na)⁺ 2887.2, (M+K)⁺ 2903.5.

2 yield 43% of a yellow oil; $^1\text{H-NMR}$ (250 MHz, CDCl_3 , δ , ppm) 8.84 (d, 2Ar-H, 8.7 Hz), 8.24 (s, 2Ar-H), 8.07-7.78 (m, 20Ar-H), 7.65 (d, 4Ar-H, *m* to OCH_2 , 8.5 Hz), 6.86 (m, 8Ar-H), 4.04 (d, 8H, $4 \times \text{CH}_2\text{Ophenyl}$, $J = 4.9$ Hz), 3.85-3.42 (m, 240H, OCH_2), 3.34 (m, 48H, OCH_3), 2.52-2.28 (m, 4H, $\text{phenylOCH}_2\text{CH}(\text{CH}_2\text{O})_2$), 2.26-1.94 (m, 8H, $8 \times \text{CH}(\text{CH}_2)_3$), 1.13–1.08 (m, 48H, $16 \times \text{CHCH}_3$); $^{13}\text{C-NMR}$ (60 MHz, CDCl_3 , ppm) : = 157.9, 142.3, 139.9, 139.8, 139.6, 132.5, 132.4, 128.6, 127.8, 127.6, 127.4 126.5, 120.0, 117.5, 108.3, 95.3, 75.0, 71.9, 70.6, 70.5, 69.6, 69.4, 67.4, 66.6, 58.9, 40.8, 17.1; Anal. Calcd for $\text{C}_{164}\text{H}_{248}\text{N}_2\text{O}_{52}$: C, 63.56; H, 8.78; N, 0.62. Found C, 63.24; H, 8.80; N, 0.66. MALDI-TOF-MS

m/z (M+H)⁺ 4498.5, (M+Na)⁺ 4423.0, (M+K)⁺ 4539.3.

Dynamic Laser Light Scattering Experiments

The dynamic light scattering (DLS) experiments were performed with the aqueous solutions of dumbbell-shaped molecules **1** and **2** (0.01 wt%) at a scattering angle of 90 ° at 30 °C, using a UNIPHASE He–Ne laser operating at 632.8 nm. The maximum operating power of the laser was 30 mW. The detector optics employed optical fibers coupled to an ALV/SOSIPD/DUAL detection unit, which employed an EMI PM–28B power supply and ALV/PM–PD preamplifier/discriminator. The signal analyzer was an ALV5000/E/WIN multiple tau digital correlator with 288 exponentially spaced channels.

LCST Measurements

Lower critical solution temperatures (LCSTs) of **1** and **2** were determined as an onset of the transmittance decrease with increasing temperature. The optical transmittances of aqueous solutions at various temperatures were recorded at wavelength of 500 nm with a Shimadzu 1601 UV-vis spectrometer (Kyoto, Japan). The sample quartz cell was thermostated with an external water bath of a Daehan Scientific precision digital refrigerated circulator (Seoul, Korea). The rate of temperature increase was 0.3 °C / min. At each temperature, the solutions were equilibrated for 10 minutes.

FRET (fluorescence resonance energy transfer)

As the emission of molecule **1** showed a significant overlap with the absorption of Nile Red dye (Figure S5), we selected Nile Red for efficient FRET experiments with **1**. To intercalate Nile Red within the π - π stacked aromatic rods, **1** ($c = 3.6 \times 10^{-5}$ M in aqueous solution) added to 1 equiv Nile Red in 5 ml vial, and then the mixture was treated by ultrasonication for 30 min at 60 °C. After this time, the intercalation of Nile Red was confirmed by using fluorescence spectroscopy. As shown in Figure S4b, when the solution was excited at 355 nm, the fluorescence spectra of **1** ($c = 3.6 \times 10^{-5}$ M) showed only a strong emission at 425 nm, suggesting that intercalation did not occur. However, while cooling from 60 to 30 °C, the fluorescence significantly quenched at the emission of 425 nm with concurrent formation of the emission at 620 nm corresponding to the Nile Red dye, indicating the occurrence of FRET from the intercalation of the Nile Red within the aromatic stacking.

TEM experiments

Transmission electron microscopy observation was carried out with a JEOL JEM–2010 operated at 120 kV. For study of structure of dumbbell-shaped molecule in aqueous solution, a drop of aqueous solution of dumbbell-shaped molecule (0.01–0.1 wt%) was placed on a carbon-coated copper grid and the solution was allowed to evaporate under ambient conditions. The samples were stained by depositing a drop of uranyl acetate aqueous solution (2 wt%) onto the surface of the sample-loaded grid.

The cryogenic transmission electron microscopy (cryo-TEM) experiments were performed with a thin film of aqueous solution of dumbbell-shaped molecule (5 μ l) transferred to a lacey supported grid. The thin aqueous films were prepared under controlled temperature and humidity conditions (97–99 %) within a custom-built environmental chamber in order to prevent evaporation of water from sample solution. The excess liquid was blotted with filter paper for 2–3 seconds, and the thin aqueous films were rapidly vitrified by plunging them into liquid ethane (cooled by liquid nitrogen) at its freezing point. To investigate the effect of temperature, solution was sealed with Teflon tape and elevated the desired temperature in Daehan Scientific precision digital refrigerated circulator having an accuracy ± 0.1 $^{\circ}$ C. The system was maintained for 1 h. And then solution was placed on the lacey supported grid, and thin aqueous films were quickly quenched in liquid ethane. The grid was transferred, on a Gatan 626 cryoholder, using a cryo-transfer device. After that they were transferred to a JEM-2010 TEM. Direct imaging was carried out at a temperature of approximately -175 $^{\circ}$ C and with a 120 kV accelerating voltage, using the images acquired with a Dual vision 300 W and SC 1000 CCD camera (Gatan, Inc.; Warrendale, PA)

Supporting Figures

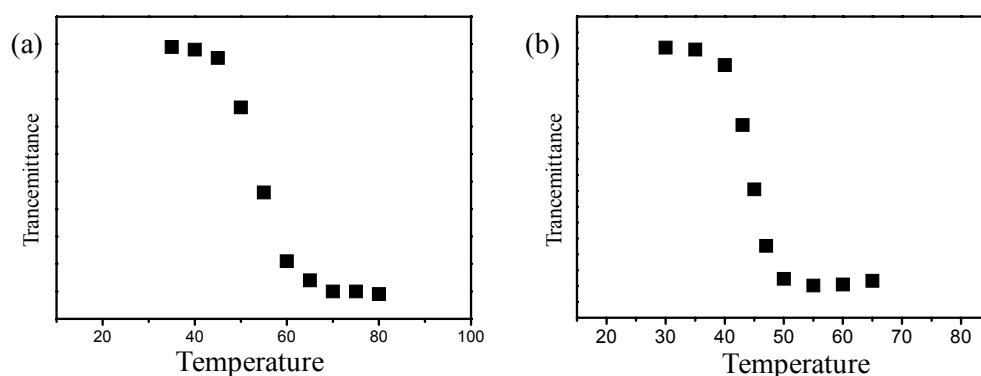


Figure S1. Transmittance measurement for (a) **1** and (b) **2** in aqueous solution (0.05 wt%) at 500 nm wavelength.

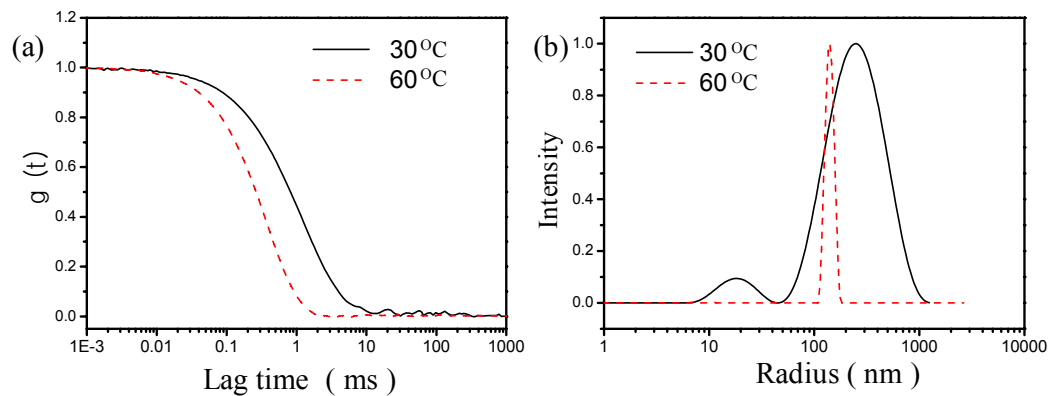


Figure S2. (a) Autocorrelation functions and (b) Size distribution graph (at a scattering angle of 90° from CONTIN analysis) of **1** in aqueous solution (0.01 wt%) at different temperatures.

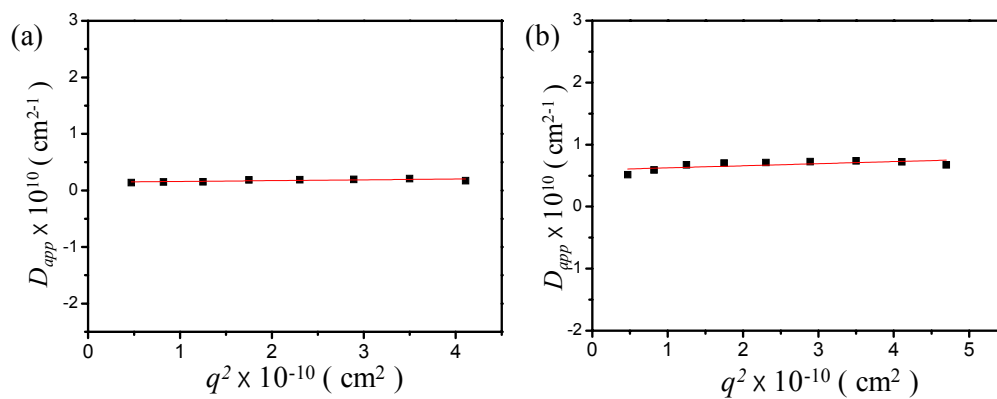


Figure S3. Angular dependence of diffusion coefficient for **1** (a) at 30 °C and (b) at 60 °C and the slope of 0.03 confirmed the cylindrical shape of **1** in aqueous solution.

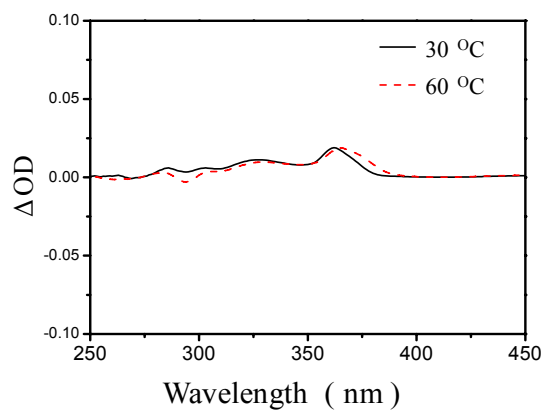


Figure S4. LD spectra of **1** (0.01 wt%) with temperature variation cooling from 60 to 30 °C.

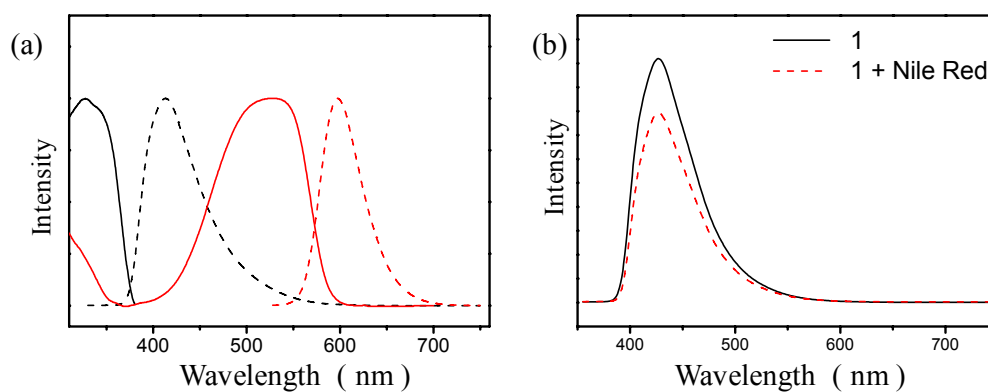


Figure S5. (a) UV-vis spectra of **1** (black solid line), Nile Red (red solid line) and fluorescence spectra of **1** (black dash line), Nile Red (red dash line) at 30 °C (excited at 355 nm for **1** and 520 nm for Nile Red). (b) Fluorescence spectra of **1** ($c = 3.6 \times 10^{-5}$ M in aqueous solution) in the absence (black solid line) and in the presence (red dash line) of 1 equiv Nile Red at 60 °C (excited at 355 nm); The FRET process does not occur, indicating that the Nile Red can not intercalate within aromatic stacking of **1** at 60 °C.

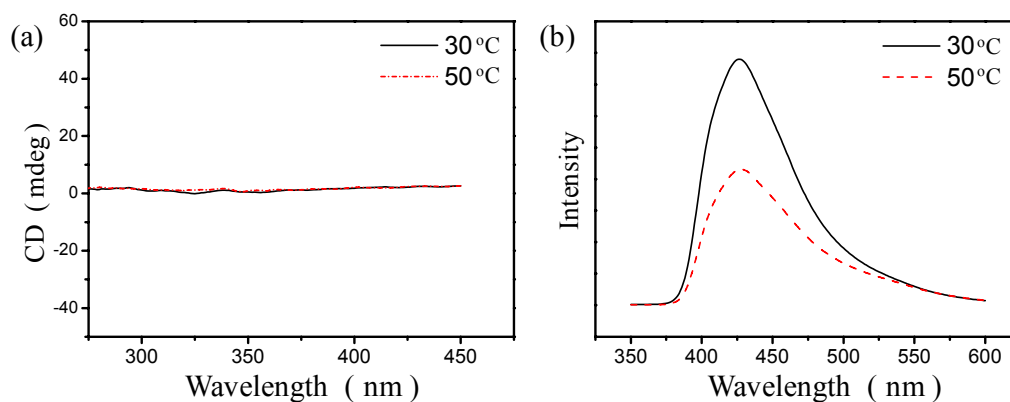


Figure S6. (a) CD spectra, and (b) fluorescence spectra of **2** (0.01 wt%) with temperature variation cooling from 50 to 30 °C.

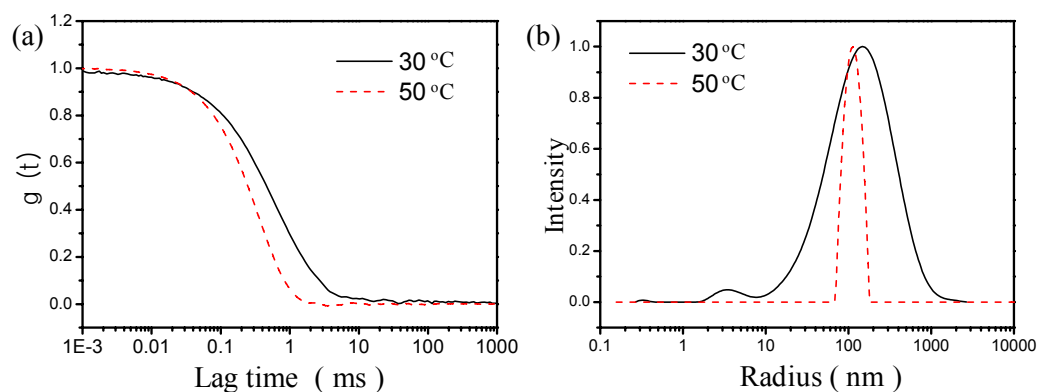


Figure S7. (a) Autocorrelation functions and (b) Size distribution graph (at a scattering angle of 90° from CONTIN analysis) of **2** in aqueous solution (0.01 wt%) at different temperatures.

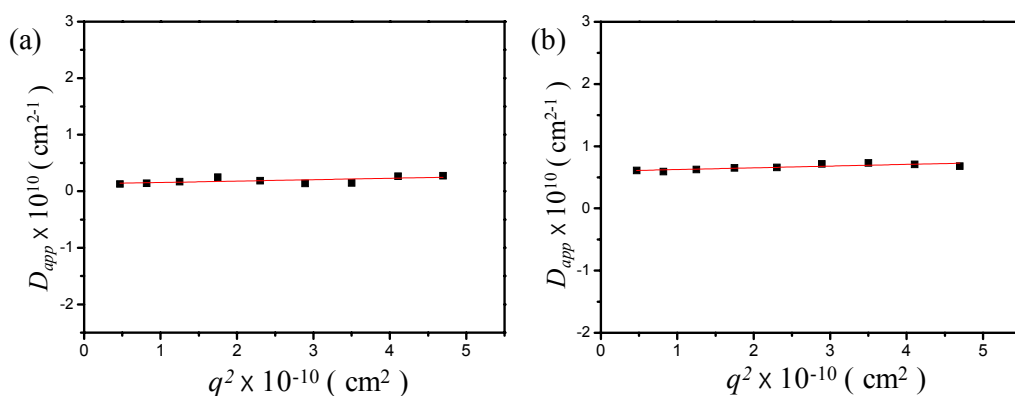


Figure S8. Angular dependence of diffusion coefficient for **2** (a) at 30 °C and (b) at 50 °C and the slope of 0.03 confirmed the cylindrical shape of **2** in aqueous solution.

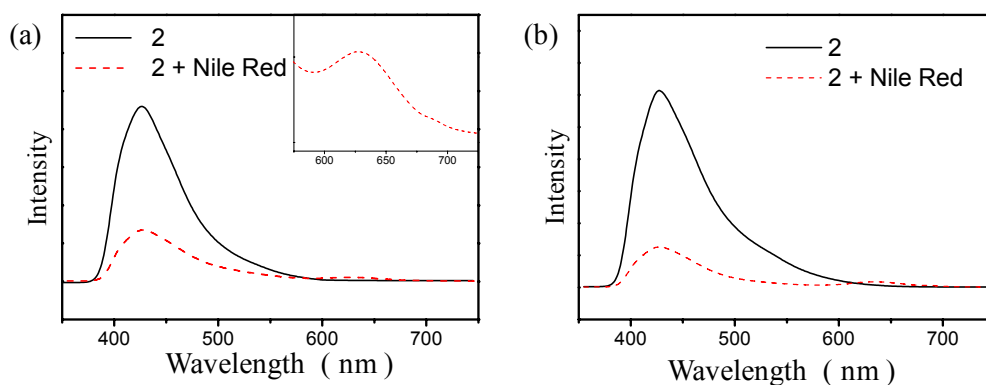


Figure S9. Fluorescence spectra of **2** ($c = 3.6 \times 10^{-5}$ M in aqueous solution) (a) at 30 °C and (b) 50 °C in the absence (black solid line) and in the presence (red dash line) of 1 equiv Nile Red (excited at 355 nm);

The FRET process occurs, indicating that the Nile Red can intercalate within aromatic stacking of **2**.

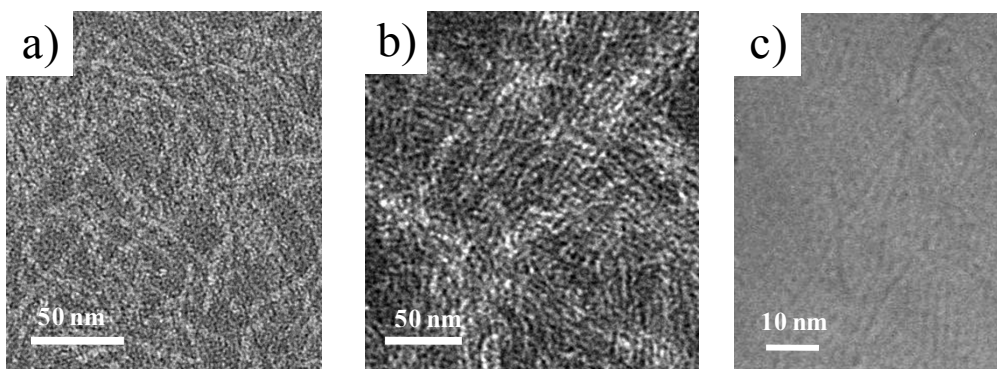


Figure S10. TEM images (negatively stained with uranyl acetate) of aqueous solutions of **2** prepared (a) at 30 °C and (b) at 50 °C. (c) A cryo-TEM image of aqueous solution of **2** prepared at 50 °C.

Reference for Supporting Information

- (1) Z. Huang, J.-H. Ryu, E. Lee, M. Lee, *Chem. Mater.*, 2007, **19**, 6569.